

# A seismic reservoir characterization and porosity estimation workflow to support geological model update: pre-salt reservoir case study, Brazil

Laryssa Oliveira<sup>1\*</sup>, Francis Pimentel<sup>2</sup>, Manuel Peiro<sup>1</sup>, Pedro Amaral<sup>2</sup> and João Christovan<sup>2</sup> present an integrated study that combines geophysical and geological approaches to estimate porosity and populate the reservoir geological model.

## Introduction

Quantitative seismic interpretation plays an important and growing role for reservoir characterization, as seismic data become increasingly reliable as a result of the latest advances in acquisition and processing techniques.

With these advances, the multi-disciplinary integration between geology, geophysics and engineering becomes increasingly effective at reducing operational risks relating to reservoir exploration and production. In addition, a multi-disciplinary approach is essential for a better understanding of reservoir features.

In this paper, we present an integrated study that combines geophysical and geological approaches to perform porosity estimation and populate the reservoir geological model (static model). For pre-salt oilfields, owing to the complex porosity distribution in carbonate reservoirs, predicting a reliable porosity is a fundamental step for reservoir modelling.

After presenting some of the specific challenges associated with pre-salt reservoirs, we will describe pre-stack seismic data preconditioning. This first step is important to improve the seismic data set at the target level in terms of signal-to-noise ratio and resolution before it is used as input to seismic inversion, the second step in this workflow. In the seismic inversion process, reservoir elastic properties are estimated. From these inverted elastic properties, it is possible to perform a Bayesian lithofacies classification and, as the final products for this step, litho-probability volumes are generated in co-operation with the field's geologists to be subsequently used as input to the geological modelling.

For the third and last step, we used facies probability volumes and acoustic impedance to estimate porosity. To use probability volumes in porosity model building, we designed a workflow to transform probability values into 3D porosity trends: first, a categorical facies volume is created by applying cut-offs on lithofacies probability volumes. For each layer of this model, a mean porosity per categorical region (facies), based on porosity logs at wells is calculated. Then, a relationship between acoustic impedance and mean porosity values was determined to create the final trend porosity volume to guide the porosity prediction away from wells.

Finally, we ran flow model simulations to quantify the benefits of the integrated workflow compared to a more commonly

used 2D porosity map-based approach, showing the improvement in matching static and dynamic reservoir properties, mainly for pressure and Gas Oil Ratio (GOR) predictions.

## Brazilian pre-salt reservoirs

Brazilian pre-salt fields are located in ultra-deep waters (around 1900 to 2400 m depth) in the Santos basin, southeast Brazil. The pre-salt area covers approximately 160,000 km<sup>2</sup> and around 20 oil fields have already been mapped since its initial discovery in 2006.

Pre-salt reservoirs are predominantly composed of lacustrine carbonates, especially microbialite carbonates in the higher reservoir zones (Estrella et al., 2008; Doborek, 2012) and carbonates with coquinas in the lower reservoir zones. In the lower reservoir zone, fractured volcanic rocks with some minor oil-filled porosity can also be found (Chang et al., 2008).

In general, pre-salt carbonates are very heterogeneous reservoirs, in terms of facies, and consequently, in terms of porosity and permeability. Processes such as diagenesis and recrystallization can modify the primary porosity and make the lithofacies heterogeneous. The higher reservoir zone is separated into two main groups: high-energy carbonates, composed mainly of stromatolites and grainstones, and low-energy carbonates, composed of laminites and spherulites.

Low-energy carbonates could present clay content and are associated with poor-quality reservoirs or non-reservoir. Meanwhile, high-energy carbonates present good porosity and permeability and are free of clay particles and are associated with good-quality reservoirs.

Feasibility and rock physics studies conducted on the basis of available wells (not further detailed in the present work) suggest a potentially good separation for reservoir and non-reservoir carbonate facies when crossplotting acoustic impedance ( $I_p$ ) and  $V_p/V_s$  elastic attributes as shown in Figure 1.

In this context, a reliable seismic reservoir characterization study plays an important role in pre-salt reservoir characterization by making it possible to discriminate the different carbonate lithofacies, and separate reservoir and non-reservoir intervals based on the elastic properties derived through elastic inversion using seismic data.

<sup>1</sup> CCG | <sup>2</sup> Petrobras

\* Corresponding author, E-mail: laryssa.oliveira@cgg.com

For this purpose, a specific workflow was adapted to predict reliable reservoir properties, minimizing the uncertainties associated with the seismic data and considering the high heterogeneity of pre-salt reservoirs.

**Geophysical approach: seismic preconditioning, elastic inversion and lithofacies classification**

Improving the quality of seismic data prior to starting any quantitative analysis is an important task to ensure a successful reservoir characterization study. This seismic data conditioning is performed prior to elastic inversion and focuses on the reservoir interval at reservoir scale and its main features. Also, quality control (QC) is performed after the completion of each step to monitor data improvements and ensure preservation of the Amplitude Versus Offset (AVO) response.

*Seismic data preconditioning*

In order to improve the signal-to-noise ratio, seismic amplitude reliability and vertical resolution in the reservoir interval, we designed a specific data preconditioning workflow for the

depth-migrated input gathers. The application of pre-stack and post-stack processes helped to mitigate the effects on seismic amplitudes of the salt layer located above the main reservoir.

This sequence involves processes such as noise attenuation and an increase in vertical resolution performed in the pre-stack and post-stack domains.

In the pre-stack domain, steps such as muting from incident angles and f-k filtering were performed. The f-k filtering application was effective at attenuating coherent noise present in far offsets on common image gathers (CIGs).

Structurally-conformable and inverse-Q filtering were the main steps performed in the post-stack domain. The structurally-conformable filtering (Hoerber et al., 2006) attenuates coherent noise generated by salt flanks. This kind of noise appears as vertical stripes in seismic data, that is easily removed by structural filtering owing to dip discrimination between noise and the primary signal reflection.

The amplitude absorption effects were compensated by applying an inverse-Q filter. The Q volume was defined using

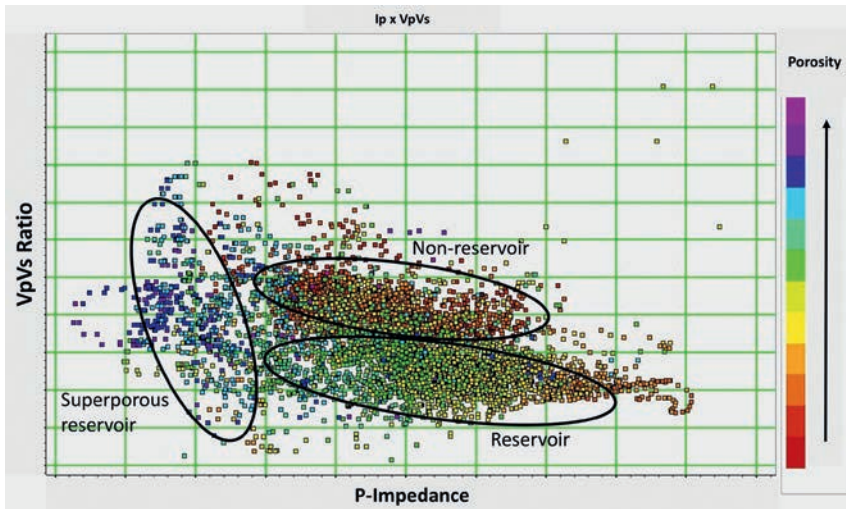


Figure 1 Crossplot of  $I_p$  vs.  $V_p/V_s$  ratio for a pre-salt reservoir oilfield.

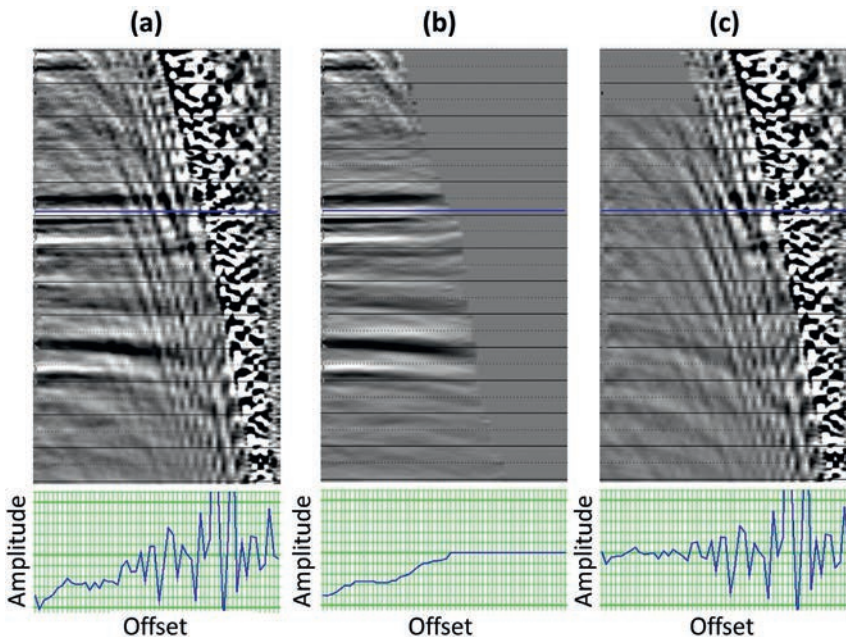
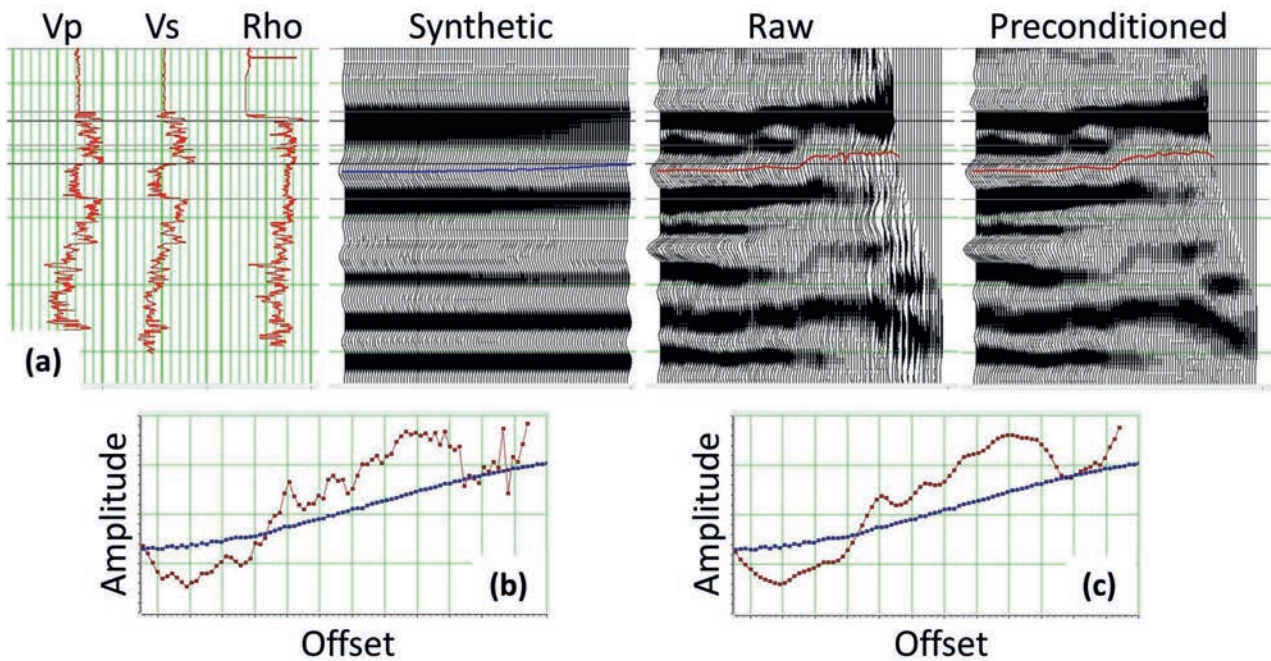
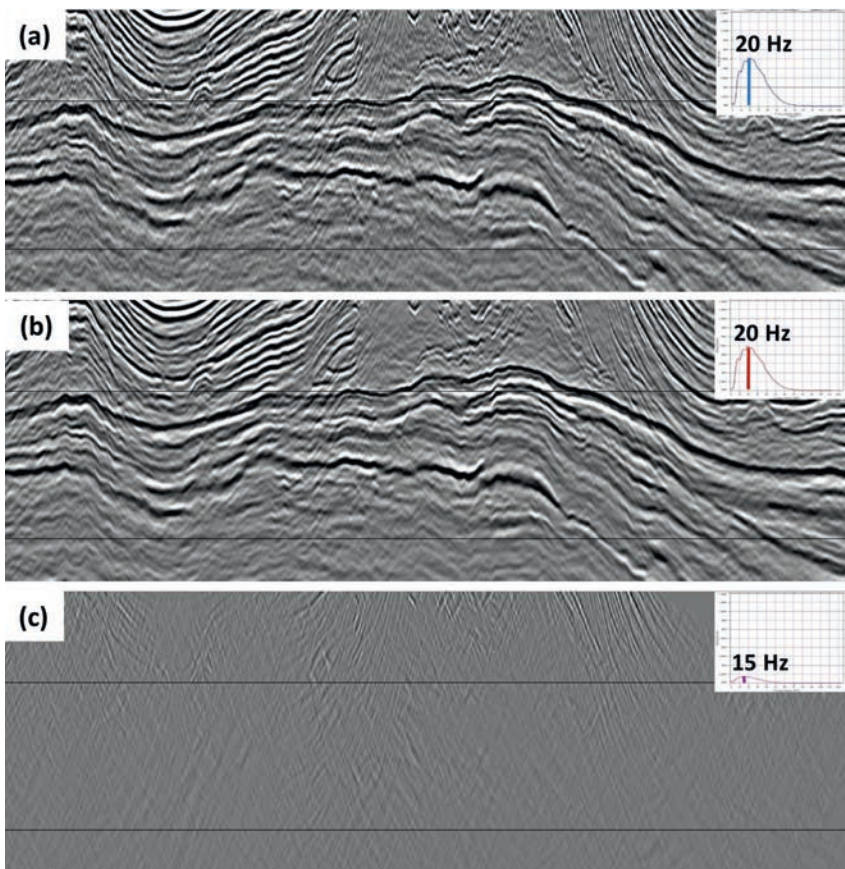


Figure 2 Gather displays and associated AVO plots used for QC during the pre-conditioning. (a) Raw gather, (b) gather after pre-stack filtering processes, (c) difference between (a) and (b).



**Figure 3** Well-tie AVO QC showing (a) AVO modelling from well logs, raw gather and the gather after pre-stack preconditioning, (b) AVO curve from synthetic (blue) and raw gather (red), and (c) AVO curve from synthetic (blue) and pre-conditioned gather (red).



**Figure 4** Stack section QC display showing (a) mid angle stack before noise attenuation, (b) mid angle stack section after noise attenuation, and (c) Difference between (a) and (b). The average extracted seismic wavelet amplitude spectrum is also displayed along with its dominant frequency for comparison.

regional surfaces such as water bottom, salt top and salt base. The Q factor values estimated using data from vertical seismic profiles (VSP) was used to fill the stratigraphic model built from the available horizons. By doing so, we created a 3D factor Q volume to be used during the amplitude deabsorption correction.

Finally, we applied a time misalignment correction to remove residual time shifts that could remain between angle stacks. This procedure is important before the inversion process as time misalignment between angle stacks implies a wrong estimation of the AVO gradient and has a direct impact on the Vp/Vs estimation during elastic inversion.

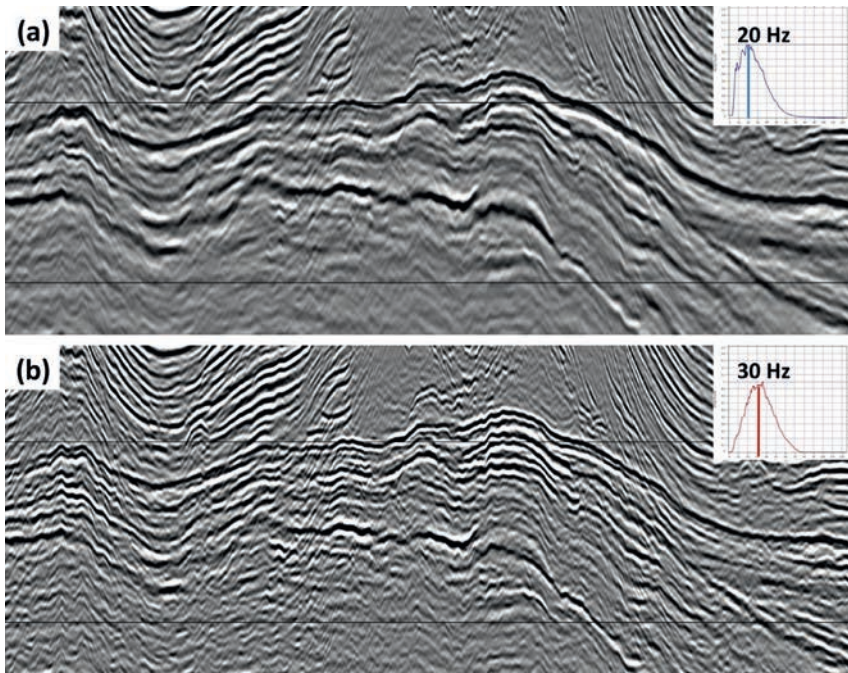


**Figure 5** Stack section inversion Q filtering QC showing (a) a mid-angle stack (a) before and (b) after inverse Q filtering. The average extracted seismic wavelet amplitude spectrum is also displayed along with its dominant frequency for comparison.

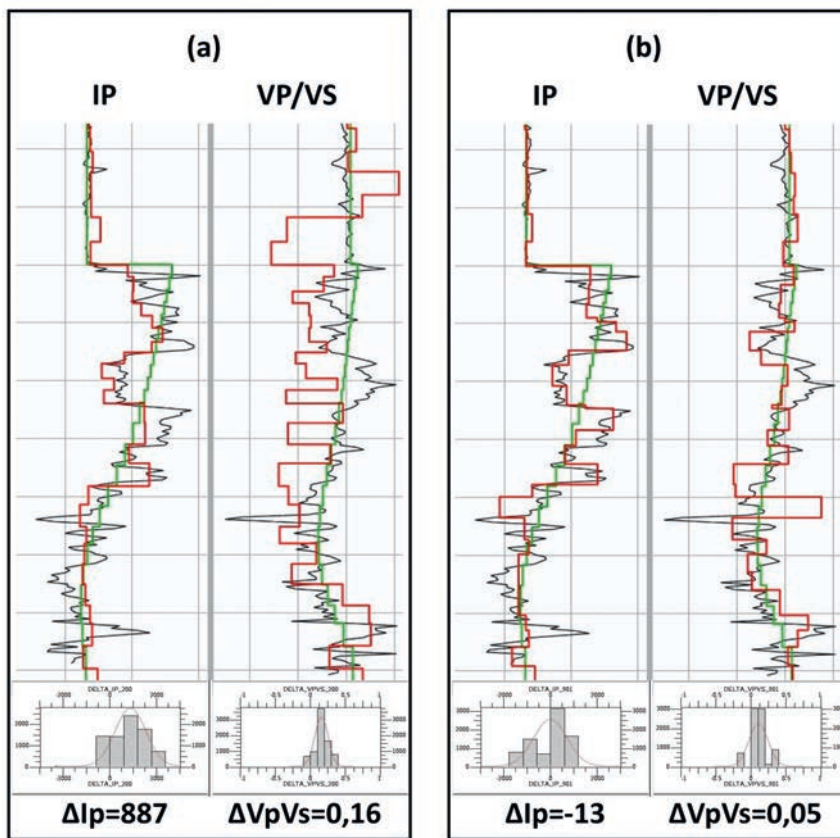


**Figure 6** Inversion well-tie QC showing well log (black), initial model (cyan) and inversion result (red), (a) before and (b) after preconditioning. Also displayed is a histogram of the mis-tie between inversion result and well log.

Stringent QC steps must be performed during pre-conditioning, in particular, to ensure preservation of the AVO response for primary reflection after each step. Using the available well data as support, each step and its impact on the AVO response was carefully analysed. AVO modelling was performed to compare the real and synthetic AVO response.

Figure 2 shows the results from all the pre-stack preconditioning processes and Figure 3 shows a comparison between the

synthetic gather, generated by AVO modelling from well logs, and the raw and pre-stack preconditioned gather. This result shows that the AVO gradient was preserved and the AVO curve is more stable, without losing frequency content.

In addition to the AVO QC for each preconditioning step, QC was performed on sections crossing through key wells. Figure 4 displays the post-stack filtering results showing mid-angle stack sections. After removal of the linear dipping noise, the

lateral continuity is improved. The results from inverse Q filtering are presented in Figure 5. From these results, it is possible to observe the dominant frequency increase, providing an enhancement in seismic resolution.

The final type of QC we performed to monitor the improvement in seismic data quality during pre-conditioning is elastic inversion, applied on a small area around key control wells. We generated five angle stacks from each preconditioning step, with a minimum and maximum angle of incidence of 5° and 45°, respectively.

The QC at the well shows clearly that the inversion results from the preconditioned data are much better, yielding

excellent estimates of  $I_p$  and a more stable  $V_p/V_s$  Ratio (see Figure 6).

*Elastic inversion*

This section shows elastic inversion results and lithofacies classification performed over a pre-salt carbonate field, highlighting how these results aggregate information for reservoir characterization and geological modelling.

The 3D, multi-cube simultaneous inversion scheme starts from an initial layered elastic model defined in the time domain (Coulon et al., 2006). During inversion, the initial model is perturbed by multiple iterations using a simulated

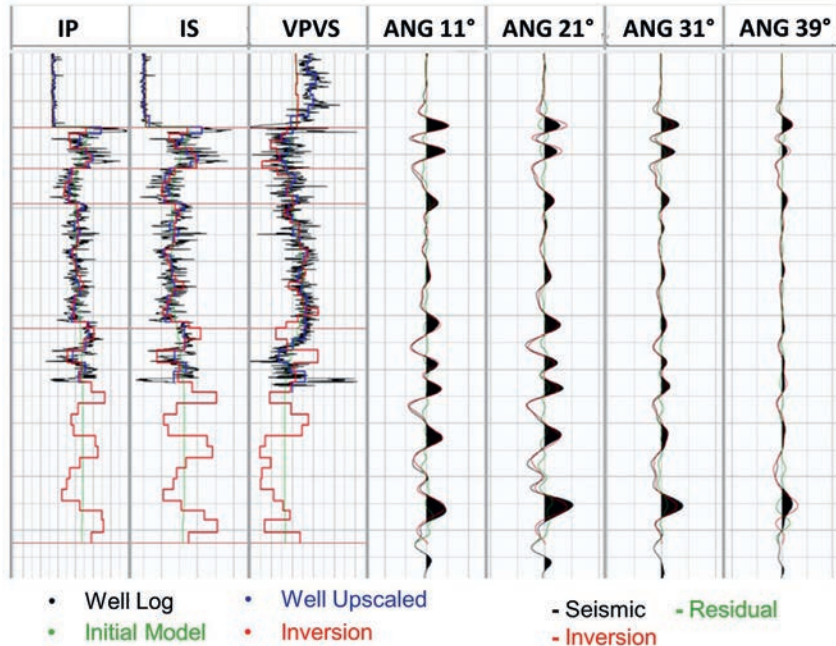


**Figure 7** Inversion QC at the well showing the comparison of inversion results to upscaled well logs for  $I_p$ ,  $I_s$  and  $V_p/V_s$  ratio and the comparison of synthetic traces from the inversion to the input seismic traces from the four angle stacks.

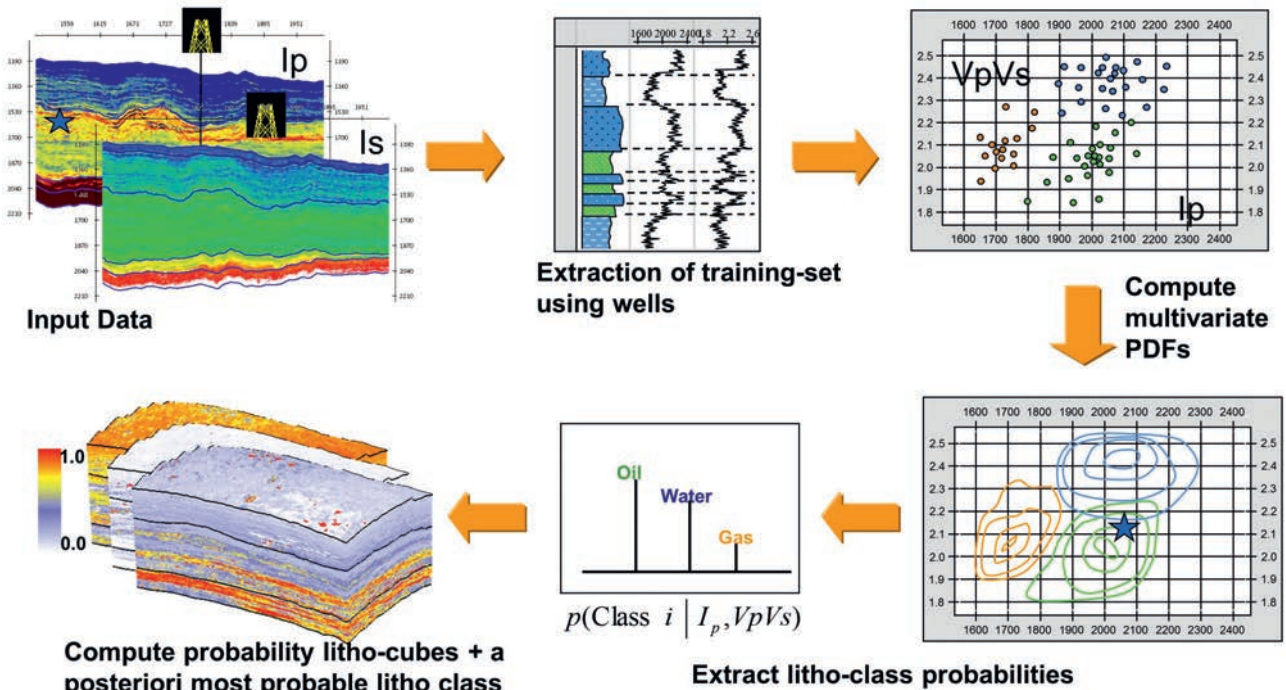


**Figure 8** Workflow for the Bayesian lithofacies classification.

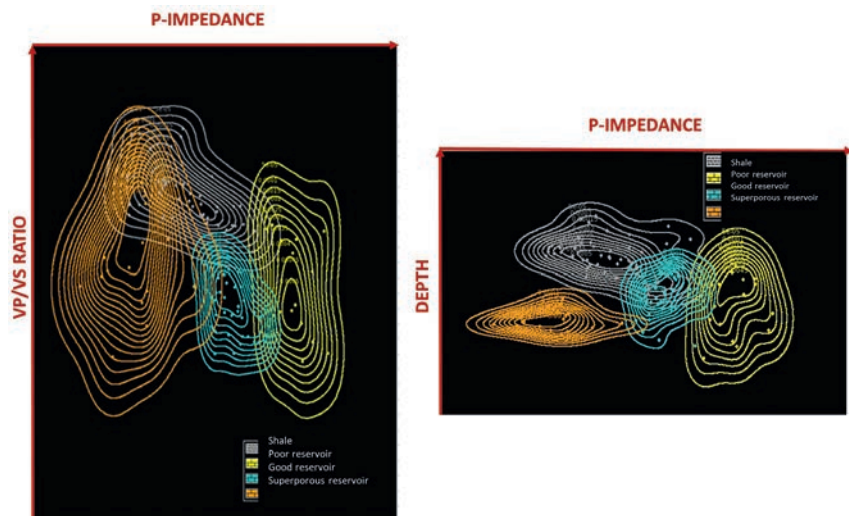
annealing procedure to find a global solution that optimizes simultaneously the match between the five input angle stacks and the corresponding synthetics calculated by convolution with full Zoepritz reflectivity equations. In addition to the data mismatch term, the objective function contains 3D spatial continuity constraints that are used to attenuate the effects of random noise. The inversion works by perturbing  $V_p$ ,  $V_s$  and density in each cell of the 3D stratigraphic grid. During inversion, independent perturbations of the different elastic parameters can be applied or perturbations can be coupled via correlations between  $V_p$ - $V_s$  and  $V_p$ -density. In addition to updating the elastic parameters, the time-thickness of the micro-layers is also adjusted during the inversion process in order to maximize the coherence between the observed seismic events and the inversion layer framework.

Figure 7 shows the inversion results at a well location. The black line is the original well log; green, the well log upscaled to the stratigraphic grid resolution; and red, the inversion results. With respect to the seismic traces, the black trace is the input (real) seismic trace; red, the synthetic trace created

from the inversion results. The comparison between upscaled blocky well log and blocky inversion results demonstrates that the inversion provided good estimates of the  $V_p/V_s$  ratio with a good decoupling between  $I_p$  and  $I_s$ . Despite the definition and inclusion of an ultra-far angle stack ( $\sim 45^\circ$ ), the inverted density cube obtained for this carbonate reservoir was difficult to stabilize and was not considered as a reliable input for the Bayesian lithofacies classification.

*Lithofacies classification*

Following the inversion process, we apply a Bayesian classification technique to these results to generate lithological probability cubes from seismically derived impedance and from lithological classification at the wells. These models are consistent with the seismic information and at the same time reproduce a priori information in the form of spatial geostatistical distributions between lithological classes. Using Bayes's theorem, the elastic properties derived from seismic observations, the prior information from well logs and the geological knowledge are all combined to define a posterior probability distribution



**Figure 9** Definition of the lithofacies classes using bivariate PDF's (contoured regions) fitted to the well log training data (points).

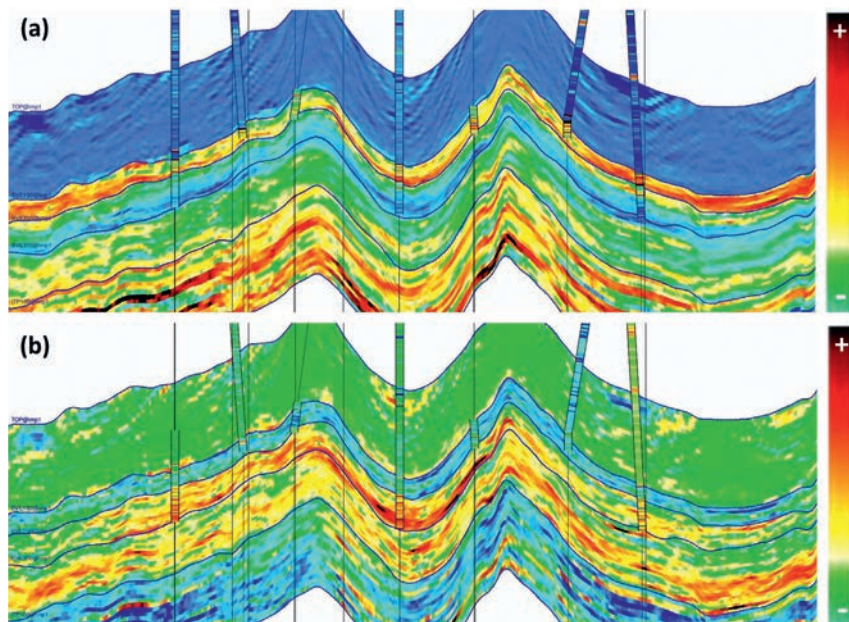


**Figure 10** Inversion QC along a section crossing eight wells. (a) Upper section corresponds to  $I_p$  attribute (b) lower section corresponds to  $V_p/V_s$  attribute.

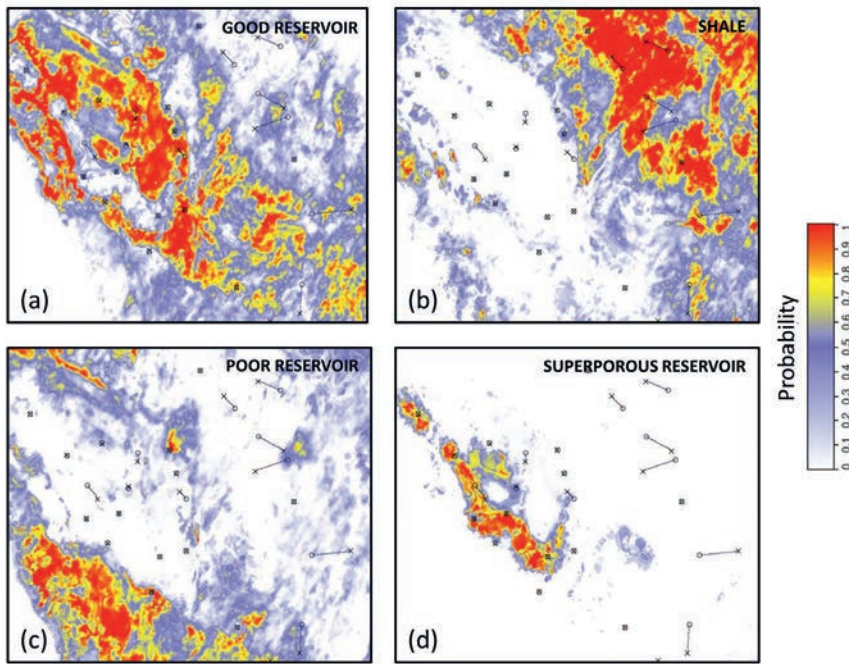


**Figure 11** Litho-probability maps corresponding to (a) good reservoir, (b) shale, (c) poor reservoir and (d) super-porosity reservoir.

function for the lithological models. The technique constructs multivariate probability density functions (PDF's) from the well logs or upscaled well logs for each litho-class that are to be predicted. Well data (facies interpretation and elastic logs) are used to build a training set for the classification. Log data points in the training set are displayed in a series of 2D cross plots of elastic attributes. Next, a multivariate PDF is fitted to each cluster of points in the training set using a non-parametric modelling technique. The PDFs are then applied to the elastic inversion results to calculate litho-probability cubes that can be used for risk assessment when planning new well locations. Figure 8 shows the workflow of this methodology.

Furthermore, a priori information about lithofacies proportions, for different regions (e.g., according to production zones, geological units) inside the reservoir, could be used to control the lithofacies distribution over the area of interest taking into account the conceptual geological model. Using this information, litho-probability cubes and a most probable lithology cube are computed based on the a priori facies proportions.

For this study, four lithofacies were defined at well locations: shale, good reservoir, bad reservoir and super-porosity. The Bayesian classification takes as input three attributes:  $I_p$ ,  $V_p/V_s$  ratio and depth. We construct 2D crossplots combining these attributes at wells and the PDFs were estimated for each lithology class as illustrated in Figure 9. The good separation between PDFs ensured that we obtained higher-probability lithofacies cubes, reducing the uncertainty of the seismic lithology prediction.

As mentioned before, accurately estimating elastic properties through simultaneous elastic inversion and predicting lithofacies distribution by Bayesian classification are the main objectives for this geophysical approach to pre-salt carbonate reservoir characterization.

As shown in Figure 10, we can observe a good match between inversion results and wells logs with  $I_p$  (a) and  $V_p/V_s$  (b) elastic

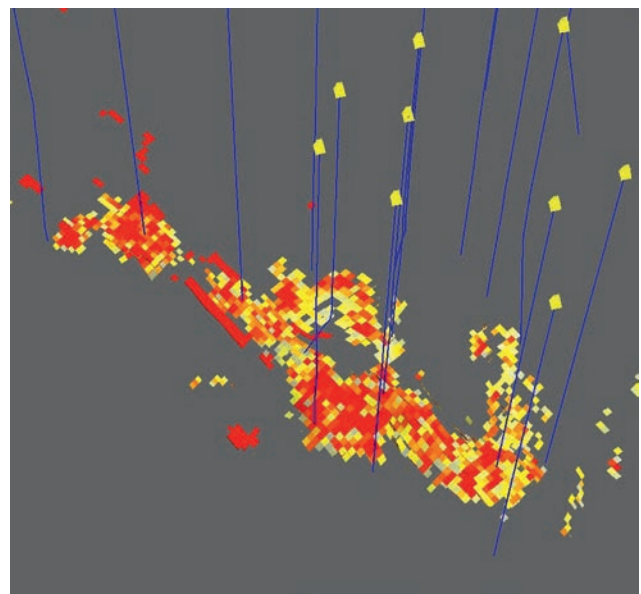


**Figure 12** 3D geobody extracted from the super-porosity probability volume.

attributes. The  $V_p/V_s$  attribute is stable and this is thanks to the rigorous pre-conditioning step applied to the seismic data.

Bayesian lithofacies classification using these inversion results provided final probability volumes for each lithofacies and these final products are illustrated in Figure 11.

According to the results, we observe the predominance of good reservoir facies in the central area, shale content concentration located on the basal portion, particularly associated with structural low and in minor occurrence, and some poor reservoir facies in the southwest area.

We also see the superporosity reservoir facies is highlighted in the NW-SE direction, encompassing the best producer wells for this pre-salt field. In this region, the effective porosity could reach values of more than 20%.

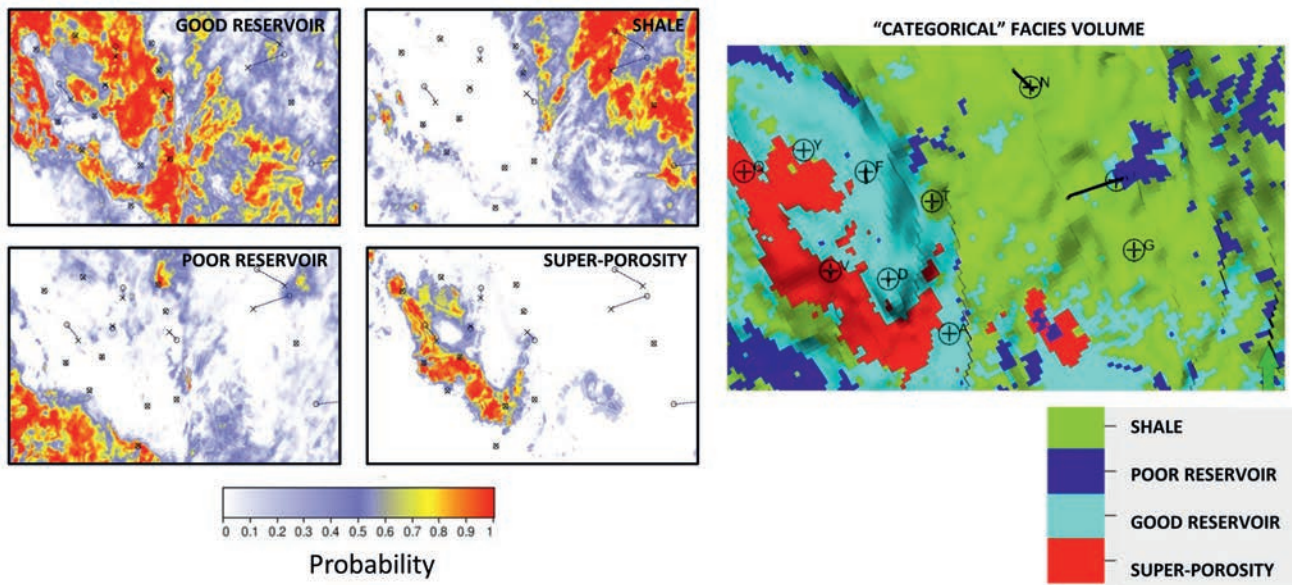


Figure 13 Extracted horizon through the 'categorical' facies volume, defined as the most probable lithofacies.

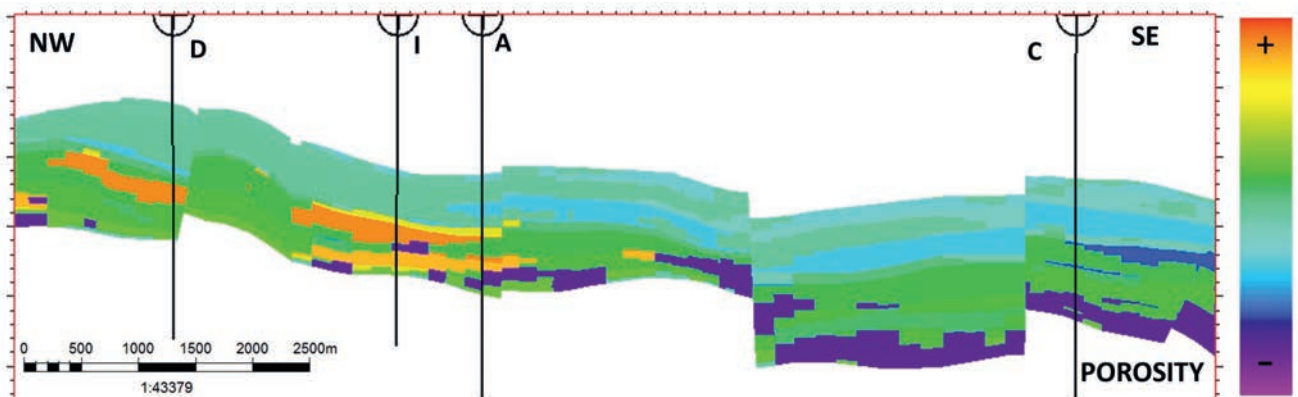


Figure 14 2D section through the 'categorical' porosity volume.

Figure 12 shows a geobody extracted from the super-porosity probability volume applying a cut-off of 80% lithofacies probability.

The 3D geobody shows the lateral and vertical distribution of the superporosity facies, crossing some wells. This lithofacies is characterized by grainstones and stromatolites with vugular porosity.

**Geological model building: porosity estimation using lithofacies volumes**

The geological model describes the main lithostratigraphic processes and provides valuable information (such as porosity and permeability) for reservoir static model building which is used as input for reservoir modelling and for each stage of reservoir development. The static model is updated as needed to refine all subsequent modelling steps.

Porosity is one of the most important properties to be predicted from the geological model, because it is strictly related to reservoir quality and potential production, and can also be related to elastic properties. In general, to fill in the porosity values inside the geological model, geologists rely on the support of seismic inversion, specifically for acoustic impedance estimation.

At well locations, well logs are available to predict the porosity, such as neutron-porosity or magnetic resonance, where effective and free-fluid porosity is predicted. These measurements are very reliable at well scale. However, additional information is needed to model the porosity away from the well locations – where the seismic data (and derived acoustic impedance) can be used to guide the porosity estimation.

Crossplotting impedance vs effective porosity from well logs makes it possible to establish a relationship between these properties and apply this relationship to the inverted acoustic impedance in order to obtain an effective porosity volume. However, applying a porosity volume derived from seismic data directly to the geological model is not an easy task: the difference between the seismic and geological grid could create upscaling issues both in vertical and lateral domains.

The standard approach used in the oil industry is to compute 2D average porosity maps from the main reservoir zones to be used as an external guide for porosity estimation.

In this work, our approach goes beyond this conventional porosity estimation using only acoustic impedance. Our purpose is to use not only impedance, but facies probability volumes converted into a lithofacies volume to be used as a guide for porosity estimation.



### Porosity estimation for static model building

In this paper we propose a new approach, which involves using not only the acoustic impedance volume from the inversion but also using the previously generated facies probability cubes.

Before describing the methodology, the transfer of properties between the seismic and geological grid is an important discussion point. As we mentioned in the previous section, the seismic inversion and lithofacies classification are steps performed in the time domain and the static model is built in depth. For property transfer, the first step is to convert the probability volumes to the depth domain with the same vertical resolution as the geological grid. Then, another conversion is carried out between the seismic depth domain and the geological depth domain using the main reservoir surfaces as reference to position all reservoir zones in the same depth location. After these steps have been performed, the probability volumes can be transferred to the geological grid.

The first step in the proposed workflow is to build a 'categorical' facies volume from the probability facies volumes. This consists in establishing cut-off values on the probability cubes

for each defined facies (super-porosity, shale, good and poor reservoir) and for each zone (1 and 2). The facies volume is illustrated in Figure 13.

In the second step of the proposed workflow, the average effective porosity from nuclear magnetic resonance (NMR) well logs are calculated by facies for each layer. As a result of this step, the 'categorical' porosity volume is a volume with different porosity values (average values) by facies and by layer, as shown in Figure 14.

The 'categorical' porosity volume only represents lithofacies with a constant porosity value per layer, which does not reflect the expected horizontal variability in porosity inside the reservoir. This is updated in the third step of the workflow.

A zone-by-zone relationship between mean porosity values and acoustic impedance by region and by layer is established. The objective of this step is to create a smooth horizontal porosity variability per layer controlled by impedance. Thus, a final porosity trend volume is created for use as a secondary variable in the geostatistical modelling of porosity.

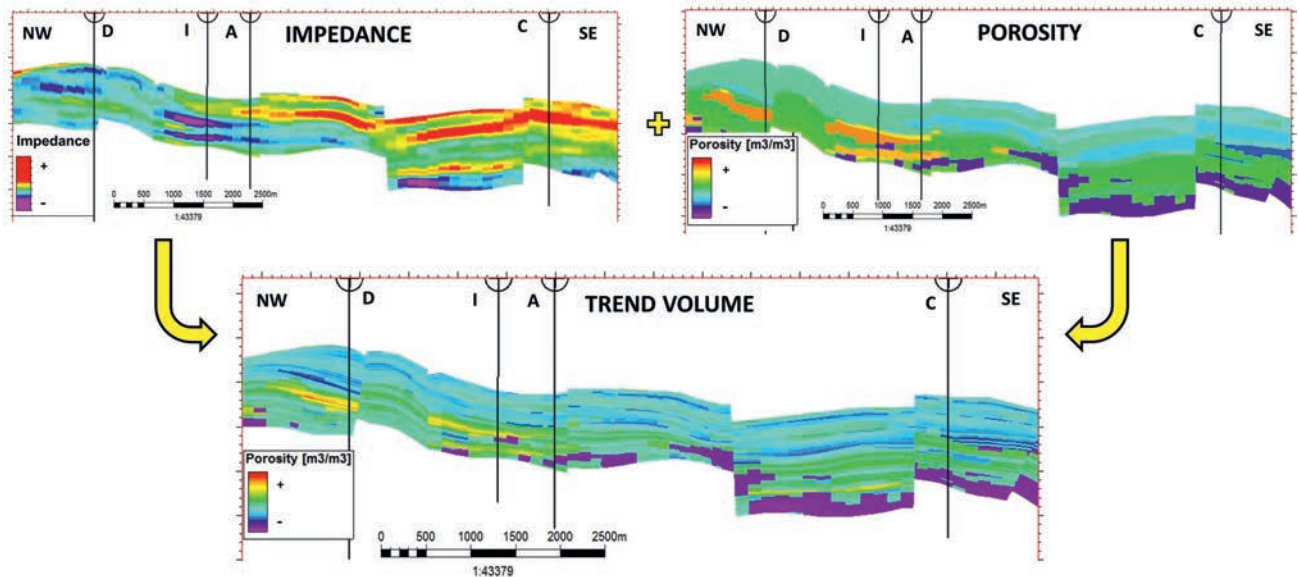


Figure 15 The porosity trend volume created using a porosity-Ip relationship to update the 'categorical' constant-value porosity model.

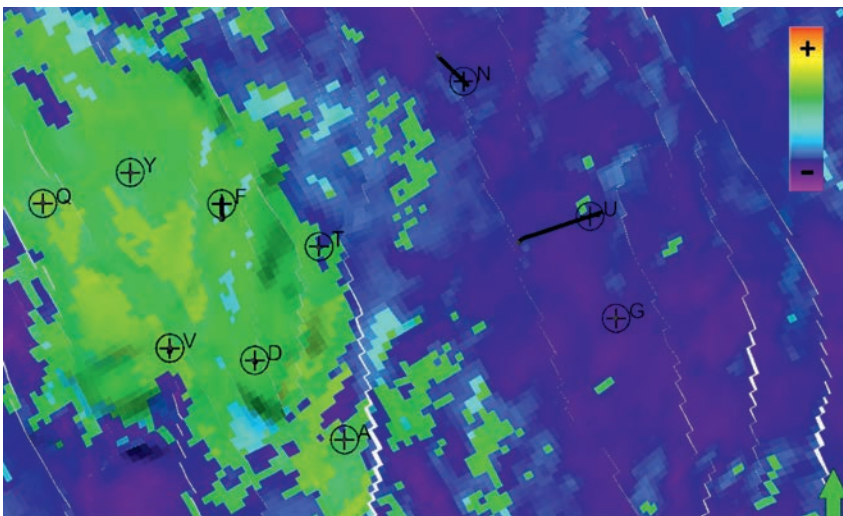
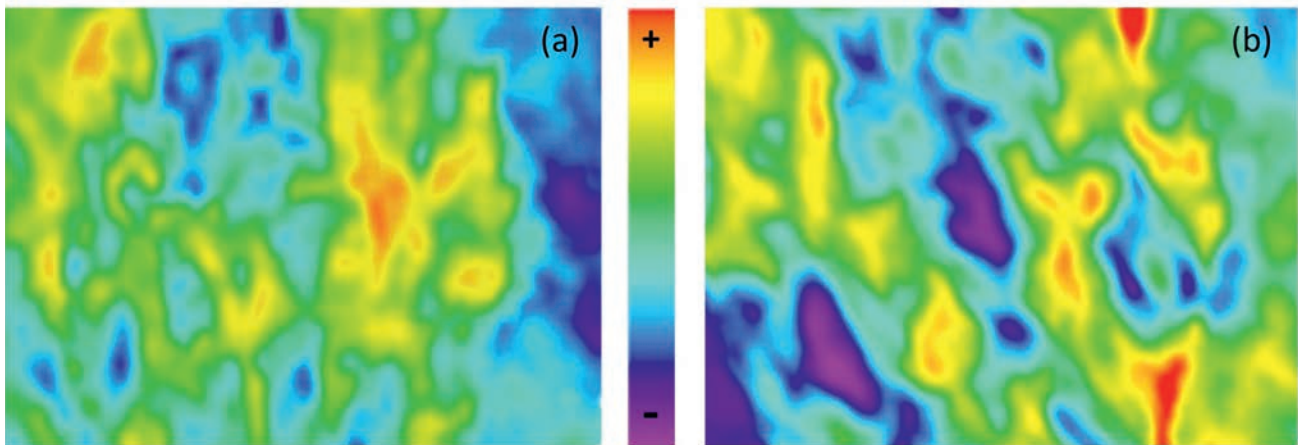
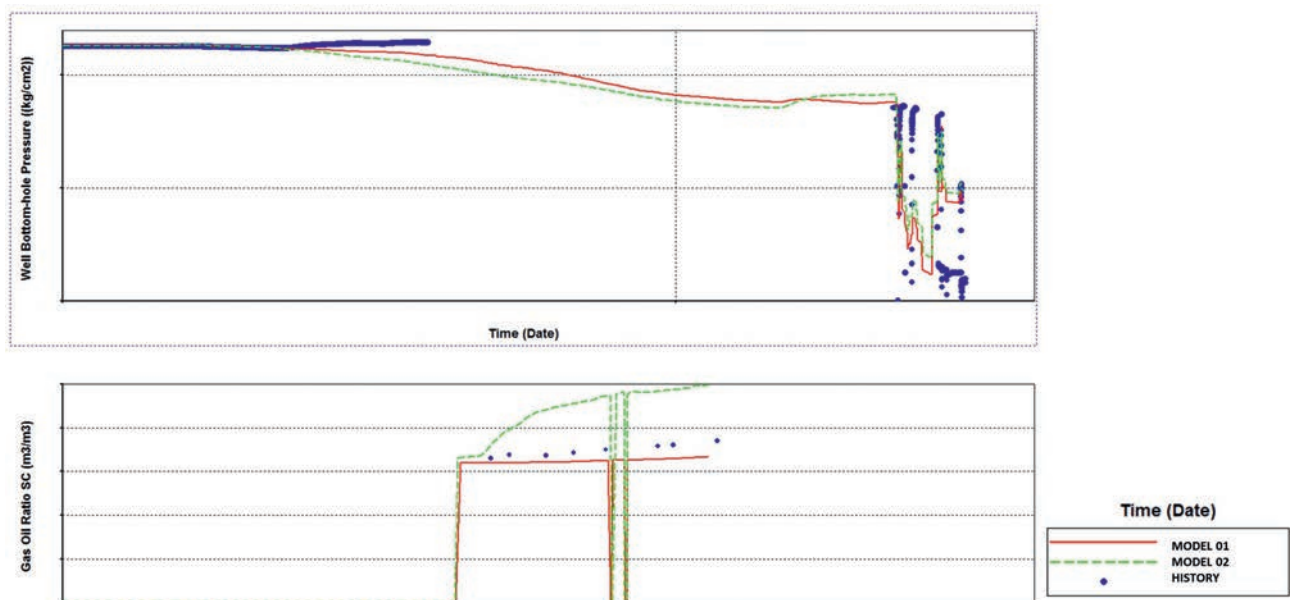


Figure 16 Porosity trend volume shown on an extracted horizon.



**Figure 17** Comparison between two porosity maps computed using two methodologies: (a) using trend porosity volume – new methodology (b) using mean porosity maps – standard approach.



**Figure 18** Comparison between simulations using two different geological models: in green (dotted line), the result using the standard method and in red, the result for the proposed methodology using the trend porosity volume.

Figure 15 illustrates the combination of the categorical porosity volume and the acoustic impedance for porosity trend volume building.

In the map for a specific layer, it is possible to see the lateral variability in the porosity values in the trend volume, as shown in Figure 16.

Average porosity maps for a reservoir zone comparing our proposed methodology to the standard procedure (using 2D mean porosity maps by zone) are illustrated in Figure 17.

For the result using the trend volume, we can observe smooth lateral continuity for the porosity model with well delineated features and variation along several azimuths. The porosity model estimated using the standard approach presents features biased along a single dominant azimuth (NW-SE) and unrealistically high lateral variability for porosity values.

It is therefore possible to infer that the use of a porosity trend volume, rather than trend maps, improves the prediction for vertical and horizontal porosity distribution, and this becomes

a more representative porosity model for the pre-salt carbonate heterogeneity facies.

In order to better quantify the value of the information brought by the integrated workflow, both versions of the porosity model (suggested workflow and commonly used trend maps) were brought to the engineering step and used for flow simulation, and the results are described in the next section.

*Validation with flow modeling simulations – engineering data*

The main function of the flow model is to be able to perform reliable predictions of well production to provide reliable revenue forecasts and support investment and decisions relating to the safety and optimization of oil and gas production.

In order to perform these tasks satisfactorily, it is essential that the simulated production data model be adjusted to the existing history data, such as the pressure of the wells (flow and static), gas/oil ratio (GOR), water percentage in the total

liquids produced (BSW), among others. For this, in addition to the adjustable parameters that are unique to the flow model, such as relative permeability curves, thermodynamic and rheological fluid properties, it is fundamental that the geological model can accurately predict the distribution of reservoir porosity and permeability.

For this pre-salt field, in particular, the GOR forecast became critical as in the early life of the field, large gas volumes had been injected generating an accelerated growth of the GOR in some wells and consequently, a possible decline in production.

By comparing GOR predictions from the proposed methodology and the standard method using mean porosity maps, we could observe an improvement in the history match using the first method in terms of its ability to honour the data of pressure and GOR for a critical well, as shown in Figure 18.

According to this analysis, in fact, the model built using the trend porosity volume presents a better match to the history of the field, recovering GOR values closer to real measurements.

### Conclusions and discussion

Brazil pre-salt carbonate reservoirs present specific challenges, combining in particular a strong heterogeneity in the reservoir facies, a complex link between the reservoir properties and elastic properties recoverable from seismic data, and a complex overburden geology that makes seismic imaging difficult. We have illustrated in this case study how combining knowledge from the various geoscience disciplines is key to reaching a realistic porosity population of the geological model, leading to a better prediction of reservoir management parameters. Starting with a tailored, reservoir-oriented pre-conditioning sequence, we optimized the input seismic data to recover reliable elastic properties during the seismic inversion. Close collaboration between geophysicists and geologists working on this field throughout the process was key to defining the facies to be discriminated during the Bayesian lithofacies classification and to check consistency of results with all previous knowledge of the field (well data, stratigraphy studies, etc.). This interaction greatly increased the ability of the geoscience team to integrate the seismic-derived cubes into the geological model porosity population. While the

use of seismic data is most commonly limited to defining 2D porosity trend maps in order to guide interpolations between wells, an advanced workflow using 3D cubes from the previous steps was designed, resulting in a porosity model consistent with geological, geophysical and well data. The improved match with the field's production history data, and GOR in particular, during reservoir simulation runs using this approach was the final step to validate the methodology and quantify its benefits from a reservoir management point of view.

### Acknowledgments

The authors would like to thank Petrobras and CGG for permission to publish this work, as well as their colleagues in both companies for fruitful discussions and valuable input during the project and the review of this article.

### References

- Chang, H.K., Assine, M.L., Corrêa, F.S., Tinen, F.C., Vidal, A.C. and Koike, L. [2008]. Sistemas petrolíferos e sistemas de acumulação de hidrocarbonetos na bacia de Santos. *Revista Brasileira de Geociências*, **38** (suplemento), 29-46.
- Coulon, J.-P., Lafet, Y., Deschizeaux, B., Doyen, P.M. and Dubois, P. [2006]. Stratigraphic Elastic Inversion for Seismic Lithology Discrimination in a Turbiditic reservoir. *76<sup>th</sup> SEG Annual International Meeting*, Expanded Abstracts, 2092-2096.
- Dorobek, S., Piccoli, L., Coffey, B. and Adams, A. [2012]. Carbonate Rock-forming Processes in the Pre-salt 'Sag' Successions of Campos Basin, Offshore Brazil: Evidence for Seasonal, Dominantly Abiotic Carbonate Precipitation, Substrate Controls, and Broader Geologic Implications. *AAPG Hedberg Conference Microbial Carbonate Reservoir Characterization*, Extended Abstracts.
- Estrella, G.O., Azevedo, R.L.M. and Formiglli Filho, J.M. [2009]. Pré-sal: Conhecimento, Estratégia e Oportunidades: Fórum Nacional/ INAE, 20, *Edição Extraordinária*, 67-78.
- Hoeber, H.C., Brandwood, S. and Whitecombe, D.N. [2006]. Structurally consistent filtering. *68<sup>th</sup> EAGE Annual Convention and Exhibition*, Expanded Abstracts.
- Scott, D.W. and Terrel, G.R. [1992]. Variable Kernel Density Estimation. *The Annals of Statistics*, 1236-1265.